



# Genetic control of susceptibility to experimental Lyme arthritis is polygenic and exhibits consistent linkage to multiple loci on chromosome 5 in four independent mouse crosses

RJ Roper<sup>1</sup>, JJ Weis<sup>2</sup>, BA McCracken<sup>1,4</sup>, CB Green<sup>1</sup>, Y Ma<sup>2</sup>, KS Weber<sup>1</sup>, D Fairbairn<sup>1</sup>, RJ Butterfield<sup>1</sup>, MR Potter<sup>2</sup>, JF Zachary<sup>1</sup>, RW Doerge<sup>3</sup> and C Teuscher<sup>1</sup>

<sup>1</sup>Department of Veterinary Pathobiology, University of Illinois at Urbana-Champaign, Urbana, IL 61802, USA; <sup>2</sup>Department of Pathology, University of Utah, Salt Lake City, UT 84132, USA; <sup>3</sup>Departments of Agronomy and Statistics, Purdue University, West Lafayette, IN 47907, USA

*C3H/He mice infected with Borrelia burgdorferi develop severe arthritis and are high antibody responders, while infected C57BL/6 and BALB/c mice develop mild arthritis and less robust humoral responses. Genetic analysis using composite interval mapping (CIM) on reciprocal backcross populations derived from C3H/HeN and C57BL/6N or C3H/HeJ and BALB/cAnN mice identified 12 new quantitative trait loci (QTL) linked to 10 murine Lyme disease phenotypes. These QTL reside on chromosomes 1, 2, 4, 6, 7, 9, 10, 12, 14, 15, 16, and 17. A reanalysis of an F<sub>2</sub> intercross between C57BL/6N and C3H/HeN mice using CIM identified two new QTL on chromosomes 4 and 15 and confirmed the location of seven previously identified loci. Two or more experimental crosses independently verified six QTL controlling phenotypes after B. burgdorferi infection. Additionally, Bb2 on chromosome 5 was reproduced in four experimental populations and was linked to the candidate locus Cora1. Evidence of four distinct QTL residing within the 30-cM region of chromosome 5 encompassing the previously mapped Bb2 and Bb3 loci was shown by CIM. Interestingly, some alleles contributing to susceptibility to Lyme arthritis were derived from C57BL/6N and BALB/cAnN mice, showing that disease-resistant strains harbor susceptibility alleles. Genes and Immunity (2001) 2, 388–397.*

**Keywords:** *Borrelia burgdorferi*; Lyme disease; arthritis; genetic control; quantitative trait loci; composite interval mapping

## Introduction

Lyme disease is the most prevalent vector borne disease in the United States.<sup>1</sup> In 1998, 16 802 cases were reported to the Centers for Disease Control and Prevention, a significant increase from the 9896 reported in 1992.<sup>1</sup> *Ixodes* ticks carry the spirochete *Borrelia burgdorferi* and pass it to humans and other mammals, with small mammals being the common reservoir hosts for the pathogen.<sup>1–5</sup>

Skin lesions (*erythema migrans*), the earliest sign of *B. burgdorferi* infection in humans, are followed by neurologic and cardiac abnormalities appearing weeks to months after infection. The most common late-stage manifestation is arthritis, with 60% of Lyme disease

patients in the United States showing symptoms 2 weeks to 2 years after infection.<sup>3</sup> The arthritis may range from intermittent episodes to chronic attacks, and the length of each relapse generally increases with the duration of illness.<sup>3,6</sup> In most individuals, the development of arthritis is associated with the presence of spirochetes in tissues.<sup>7</sup> However, approximately 10% of individuals with Lyme arthritis develop a chronic condition characterized by persistent pain in a single joint for greater than 12 months and resistance to antibiotic treatment.<sup>6</sup> This treatment-resistant disease is proposed to result from the generation of *B. burgdorferi*-specific T cells that cross react with self-antigens.<sup>8,9</sup>

Because Lyme disease shows a variety of clinical manifestations in humans it has been postulated that the immunologic and pathologic sequelae associated with infection may be under partial genetic control.<sup>3</sup> This hypothesis has been studied using mouse models of Lyme disease.<sup>10–12</sup> Susceptibility to Lyme disease differs among mouse strains: C3H/He mice, including both the C3H/HeJ and C3H/HeN substrains, inoculated with *B. burgdorferi* develop severe arthritis, C57BL/6 mice develop mild arthritis, and BALB/c mice develop a spectrum of disease, depending on the inoculum.<sup>10,13</sup> Inbred strains of mice differ in susceptibility to carditis,<sup>14</sup> antibody responses,<sup>4,5,15,16</sup> spirochete load, arthritic

Correspondence: Dr C Teuscher, Department of Veterinary Pathobiology, 2001 South Lincoln Avenue, University of Illinois at Urbana-Champaign, Urbana, IL 61802, USA. E-mail: cteusche@uiuc.edu

<sup>4</sup>Present address: Pet Products R&D, Ralston Purina Company, St Louis, MO 63164, USA.

This work was supported by NIH AR43521 (to JJW and CT). RWD was partially funded by USDA grant 98–35300–6173. RJR was partially supported by NIH Cell and Molecular Biology Training Grant T32-GM-07283. MRP was supported as a predoctoral trainee by NIH Genetics Training Grant T32-GM-07464. Core facilities at the University of Utah were supported by NIH P30-CA-42014.

Received 25 May 2001; revised and accepted 10 August 2001

**Table 1** Summary of quantitative traits associated with *B. burgdorferi* infection of parental and F<sub>1</sub> animals

Strain or cross (No. of mice)	Ankle swelling (mm)	Histo-pathology score (0–4)	Tendon sheath thickness ( $\mu$ m)	Tendon sheath histology (0–4)	Total IgM (mg/ml)	Total IgG (mg/ml)	Specific <sup>a</sup> IgM ( $\mu$ g/ml)	Specific IgG <sup>a</sup> ( $\mu$ g/ml)	I16 (ng/ml)	<i>Bb</i> copy No. in heart
C3H/HeN (10)	4.23 $\pm$ 0.23	3.7 $\pm$ 0.48	146.6 $\pm$ 60.55		1.1 $\pm$ 0.14	5.2 $\pm$ 0.47	4.5 $\pm$ 0.41	76.6 $\pm$ 12.9	3.24 $\pm$ 2.47	2117 $\pm$ 887
C57BL/6N (10)	3.01 $\pm$ 0.16	0.8 $\pm$ 0.71	67.4 $\pm$ 0.71		0.97 $\pm$ 0.18	2.9 $\pm$ 0.63	2.5 $\pm$ 1.3	43.7 $\pm$ 11.3	1.41 $\pm$ 1.51	246 $\pm$ 149
B6C3F1 (10)	3.56 $\pm$ 0.22	1.8 $\pm$ 0.86	99.0 $\pm$ 42.15		0.93 $\pm$ 0.12	3.7 $\pm$ 0.98	3.4 $\pm$ 1.2	74.69 $\pm$ 18.33	2.58 $\pm$ 2.02	464 $\pm$ 254
C3H/HeJ (42)	3.71 $\pm$ 0.27	2.08 $\pm$ 1.3		2 $\pm$ 1.3			0.63 $\pm$ 0.27	4.45 $\pm$ 2.02		
BALB/cAnN (35)	3.32 $\pm$ 0.30	1.6 $\pm$ 1.2		1.23 $\pm$ 0.91			0.36 $\pm$ 0.12	2.20 $\pm$ 0.79		
(C3H $\times$ BALB) F1 (46)	3.35 $\pm$ 0.22	1.82 $\pm$ 1		1.53 $\pm$ 0.92			0.45 $\pm$ 0.24	4.84 $\pm$ 2.10		

<sup>a</sup>The absolute values for *Borrelia burgdorferi* specific IgM and IgG presented for C3H/HeJ, BALB/cAnN and (C3H  $\times$  BALB) F1 hybrids were determined with a different ELISA assay, and cannot be directly compared with those obtained for C3H/HeN, C57BL/6N and B6C3F1 hybrid mice.

response<sup>13</sup> and T helper cell phenotypes.<sup>17</sup> However, several studies suggest a lack of involvement of acquired immunity in regulating the severity of disease.<sup>18,19</sup>

To better understand the role of genetics in the development and persistence of Lyme arthritis, our laboratories previously published the study of an F<sub>2</sub> intercross population derived from susceptible C3H/HeN and resistant C57BL/6N mice. We reported nine quantitative trait loci (QTL) linked to Lyme disease phenotypes.<sup>11</sup> Ankle swelling was associated with loci on chromosomes 4 and 5, whereas regions of chromosomes 5 and 11 were linked to arthritis histopathology. Humoral responses differing between susceptible and resistant mice were controlled by loci on chromosomes 6, 9, 11, 12, and 17.

In the present study, reciprocal backcross (BC1) populations derived from C3H/HeN and C57BL/6N, and C3H/HeJ and BALB/cAnN mice were used to further characterize the genetic control of murine Lyme disease related phenotypes (see Table 1). Using composite interval mapping (CIM), 12 new QTL from the BC1 populations and at least two new QTL from the original (C3H/HeN  $\times$  C57BL/6N) F<sub>2</sub> intercross population were identified. Importantly, CIM revealed the possibility of four loci in a 30-cM region of chromosome 5 encompassing the previously mapped *Bb2* and *Bb3* loci.

## Results

Using an F<sub>2</sub> intercross between C3H/HeN and C57BL/6N mice, we previously identified nine distinct QTL (*Bb1*–*Bb9*) governing six phenotypes associated with murine Lyme disease following *B. burgdorferi* infection.<sup>11</sup> Three QTL were associated with two different phenotypes, and five phenotypes were controlled by more than one QTL. In the present study, we analyzed *B. burgdorferi*-infected reciprocal BC1 populations, B6C3F<sub>1</sub>  $\times$  C57BL/6N and B6C3F<sub>1</sub>  $\times$  C3H/HeN, as well as (C3H/HeJ  $\times$  BALB/cAnN)  $\times$  BALB/cAnN and (C3H/HeJ  $\times$  BALB/cAnN)  $\times$  C3H/HeJ. All measurable characteristics of *B. burgdorferi* infection are similar between C3H/HeJ and C3H/HeN mice, and the two substrains develop Lyme arthritis of similar severity.<sup>13</sup> In this investigation, we

sought to identify (1) the most important QTL for Lyme disease related phenotypes, (2) additional QTL controlling *B. burgdorferi* induced phenotypes that were not found in the F<sub>2</sub> intercross, (3) QTL specific to a cross between particular parental strains, and (4) the relationship of two phenotypes that were controlled by QTL localized to a single region on the chromosome.

Because of our *a priori* knowledge of the existence of multiple QTL linked to a single Lyme disease phenotype and linkage of two Lyme disease QTL to the same chromosome,<sup>11</sup> we used CIM for this study.<sup>20,21</sup> CIM conditions out the effects of one QTL in the identification of another QTL, controls for multiple QTL on a single chromosome, and generally localizes QTL to a narrower interval. Therefore, we hypothesized that CIM would localize QTL with greater precision than traditional interval mapping in the reciprocal BC1 populations.<sup>20–24</sup> Furthermore, we hypothesized that CIM would improve our ability to distinguish QTL shared between different crosses and phenotypes from QTL that were specific to individual crosses and phenotypes.

### Quantitative analysis of severity of *B. burgdorferi*-induced arthritis based on ankle swelling and lesion scoring

When the B6C3F<sub>1</sub>  $\times$  C3H/HeN BC1 was used, QTL linked to ankle swelling and histopathologic traits reproduced *Bb2* and *Bb6* found on chromosomes 5 and 12 in the F<sub>2</sub> intercross.<sup>11</sup> Although *Bb6* was previously linked to the *B. burgdorferi* induced antibody response, in this BC1 population *Bb6* also appears to be linked to arthritis. New QTL were found centromeric of *Bb6* on chromosome 12 at 16–28 cM (*Bb10*), and on chromosome 1 at 32.8 cM (*Bb11*). (All cM references are according to Mouse Genome Database (MGD) (<http://www.informatics.jax.org/>) and are based on the distance from the centromere of the acrocentric mouse chromosome.) In the B6C3F<sub>1</sub>  $\times$  C57BL/6N BC1, *Bb2* was also verified, and new loci were linked to chromosome 1 at 92–100 cM (*Bb12*) and chromosome 4 at 6.5 cM (*Bb13*) (see Table 2).

In the (C3H/HeJ  $\times$  BALB/cAnN)  $\times$  C3H/HeJ BC1, a single QTL linked to arthritis severity based on histologic

**Table 2** Location and effects of new QTL controlling phenotypes in crosses between C3H/HeN, C57BL/6N and C3H/HeJ, BALB/cAnN mice

QTL designation	Cross <sup>a</sup>	Phenotype	Chr	cM <sup>b</sup>	Marker <sup>c</sup>	LRT <sup>d</sup>	A <sup>e</sup>	Var <sup>f</sup>
Bb2	C3H, B6	Ankle swelling	5	66–81	D5Mit431–D5Mit101	31.7	0.23	12.0
	C3H, B6	Histopathology	5	66–78	D5Mit431–D5Mit98	20.8	0.61	8.8
	B6, C3H	Tendon sheath	5	70	D5Mit214	16.1	-50.2	12.9
	C3H, BALB	Ankle swelling	5	72	D5Mit30	47.1	0.28	29.0
	C3H, BALB	Histopathology	5	56–78	D5Mit115–D5Mit31	33.4	1.15	20.6
Bb6	C3H, BALB	Tendon histology	5	58–72	D5Mit239–D5Mit30	24.7	1.09	16.0
	C3H, B6	Tendon sheath	12	45–46	D12Mit194–D12Mit121	34.1	67.9	18.9
Bb8	C3H, B6	Total IgG	12	46–52	D12Mit121–D12Mit139	28.8	492.3	11.3
	C3H, B6	Specific IgG	17	10–23.3	D17Mit46–D17Mit215	40.2	876.6	14.0
Bb10	C3H, B6	IL6	17	10–23.3	D17Mit46–D17Mit215	35.4	1316.1	14.3
	BALB, C3H	Ankle swelling	17	22.5	D17Mit176	14.5	-0.19	11.3
	BALB, C3H	Specific IgG	17	24.5	D17Mit10	12.8 <sup>g</sup>	0.92	9.7
	C3H, B6	Tendon sheath	12	16–28	D12Mit46–D12Mit69	20.1	-50.4	9.6
Bb11	C3H, B6	Total IgG	12	28	D12Mit69	11.9 <sup>g</sup>	-172.6	5.2
Bb12	C3H, B6	Ankle swelling	1	32.8	D1Mit76	14.2	-0.14	5.0
	B6, C3H	Ankle swelling	1	92.3–100	D1Mit36–	25.1	0.4	15.1
Bb13	F <sub>2</sub>	Total IgG	1	92.3	D1Mit150D1Mit36	19.1	-141.6	0.8
	B6, C3H	Ankle swelling	4	6.5	D4Mit264	18.6	-0.2	10.7
Bb14	B6, C3H	Specific IgG	15	15.6–18.8	D15Mit24–D15Mit154	18.3	11.3	12.3
	BALB, C3H	Ankle swelling	15	17.8	D15Mit111	15.1	0.22	11.9
Bb15	C3H, B6	Specific IgG	2	70–74	D2Mit278–D2Mit224	14.7	12.1	5.8
	B6, C3H	Total IgG	2	74	D2Mit224	17.6	608.9	13.5
Bb16	C3H, B6	Total IgG	7	16–53	D7Mit227–D7Mit40	20.1	386.4	6.8
Bb17	B6, C3H	Specific IgG	9	56	D9Mit24	15.1	-10.4	9.9
Bb18	B6, C3H	Specific IgM	10	31.5	D10Mit130	16.7	1352.2	12.2
Bb19	B6, C3H	Specific IgG	16	9.7	D16Mit88	16.8	10.9	11.2
Bb20	BALB, C3H	Specific IgG	6	30.5–38.5	D6Mit16–D6Mit102	18.9	1.14	14.8
Bb21	B6, C3H	Bb copy in heart	14	25	D14Mit155	13.2	459.7	9.8
Bb22	F <sup>2</sup>	Histopathology	15	46.9	D15Mit24	19.8	1.0	17.3
Bb23	F <sub>2</sub>	Bb copy in heart	4	49.6	D4Mit219	21.6	525.9	11.2

<sup>a</sup>C3H, B6 = B6C3F<sub>1</sub> × C3H/HeN BC1; B6, C3H = B6C3F<sub>1</sub> × C57BL/6N BC1; C3H, BALB = (C3H/HeJ × BALB/cAnN) × C3H/HeJ BC1; BALB, C3H = (C3H/HeJ × BALB/cAnN) × BALB/cAnN BC1. <sup>b</sup>Distance according to MGD (<http://www.informatics.jax.org/>). <sup>c</sup>Marker(s) that surpass 95% permutation-based experimentwise level of significance based on 1000 permutations. For B6C3F<sub>1</sub> × C3H/HeN BC1: histopathology: 13.2, tendon sheath thickness: 13.9, ankle swelling: 12.8, specific IgG: 13.2, specific IgM: 13.4, total IgG: 13.3, total IgM: 13.4, IL6: 13.3, *B. burgdorferi* copy in heart: 12.1. For B6C3F<sub>1</sub> × C57BL/6N BC1: histopathology: 14.7, tendon sheath thickness: 15.8, ankle swelling: 14.8, specific IgG: 15.0, specific IgM: 15.3, total IgG: 14.7, total IgM: 14.9, IL6: 14.9, *B. burgdorferi* copy in heart 12.1. For (C3H/HeJ × BALB/cAnN) × C3H/HeJ BC1: ankle swelling: 12.9, histopathology: 12.72, tendon histology: 13.01; For (C3H/HeJ × BALB/cAnN) × BALB/cAnN BC1: ankle swelling: 13.9, specific IgG: 13.7. <sup>d</sup>Maximum LRT at the position of a marker (not an interval between markers). <sup>e</sup>Additive effect of the QTL relative to the C3H/HeN [in the B6C3HF<sub>1</sub> × C3H/HeN and (C3H/HeN × BALB/cAnN) × C3H/HeN crosses], C57BL/6N (in the B6C3F<sub>1</sub> × C57BL/6N cross) or BALB/cAnN [in the (C3H/HeN × BALB/cAnN) × BALB/cAnN cross] homozygote. A positive value indicates that the mean trait value for the homozygous (a marker having two alleles from the recurrent parent of the BC1) animals is greater than the mean trait value for the heterozygous animals. <sup>f</sup>Percent variance accounted for by the QTL. <sup>g</sup>90% permutation-based experimentwise significance levels. For (C3H/HeN × BALB/cAnN) × BALB/cAnN BC1: specific IgG = 11.8; For B6C3HF<sub>1</sub> × C3H/HeN BC1: total IgG = 11.9.

analysis was found in the region from 56–78 cM on chromosome 5 (*Bb2*). In the (C3H/HeJ × BALB/cAnN) × BALB/cAnN BC1, the *Bb8* locus was reproduced on chromosome 17, and a new QTL was identified at 17.8 cM on chromosome 15 (*Bb14*).

**Quantitative analysis of the humoral response to *B. burgdorferi* infection**

QTL linked to IgG or IgM antibody levels (both total and *B. burgdorferi* specific) were also found using the reciprocal BC1 populations. The B6C3F<sub>1</sub> × C3H/HeN BC1 verified *Bb6* and *Bb8* on chromosomes 12 and 17 that were previously mapped in the F<sub>2</sub> intercross, as well as the *Bb10* locus on chromosome 12.<sup>11</sup> New QTL were mapped to 70–74 cM on chromosome 2 (*Bb15*) and 16–53 cM on chromosome 7 (*Bb16*). In the B6C3F<sub>1</sub> × C57BL/6N BC1, *Bb12* on chromosome 2 was also confirmed at 74 cM, and new QTL were found on chromosome 9 at 56 cM (*Bb17*), chromosome 10 at 31.5 cM (*Bb19*), chromosome 15 at

15.6–18.8 cM (*Bb14*), and chromosome 16 at 9.7 cM (*Bb19*). A new locus at 30.5–38.5 cM (*Bb20*) on chromosome 6 was mapped in the (C3H/HeJ × BALB/cAnN) × BALB/cAnN BC1.

**Quantitative analysis of IL-6 and *B. burgdorferi* numbers in the heart**

Elevated interleukin-6 (IL-6) levels following *B. burgdorferi* infection mapped to 10–23.3 cM on chromosome 17 in the B6C3F<sub>1</sub> × C3H/HeN BC1, where *Bb8* had been previously localized.<sup>11</sup> Also, a QTL controlling the number of *B. burgdorferi* residing in heart tissues after infection was linked to 25 cM on chromosome 14 (*Bb21*) in the B6C3F<sub>1</sub> × C57BL/6N BC1.

**Composite interval mapping reanalysis of the F<sub>2</sub> intercross**

When CIM on the BC1 populations revealed many unique loci not identified in the original F<sub>2</sub> genome

scan,<sup>11</sup> we asked whether the additional QTL found in the BC1 populations, but not seen in the F<sub>2</sub> intercross, reflected the increased power of CIM to localize QTL. Utilizing markers covering the entire genome of the original F<sub>2</sub> population, we analyzed each phenotype by CIM. Twenty background markers were selected to account for the potential background effects of *Bb1*–*Bb21*. CIM confirmed *Bb1*–*Bb6* and *Bb8* (see Table 3). Additionally, *Bb12* controlling the total IgG level was verified at 92.3 M on chromosome 1. Two new QTL were identified on chromosomes with previously identified *B. burgdorferi*-associated QTL. *Bb22* mapped to 46.9 cM on chromosome 15 (histopathology) and *Bb23* at 49.6 cM on chromosome 4 (quantification of *B. burgdorferi* copy number in the heart) (see Tables 2 and 3).

### Replication of *Bb* loci between crosses

Seven QTL were replicated in multiple crosses with various phenotypes. *Bb2*, associated with histopathology, was verified in the three crosses using C3H/HeN and C57BL/6N mice and was the *only* significant QTL found in the (C3H/HeJ × BALB/cAnN) × C3H/HeJ BC1. *Bb8* was mapped in the F<sub>2</sub> intercross, the B6C3F<sub>1</sub> × C3H/HeN BC1, and the (C3H/HeJ × BALB/cAnN) × BALB/cAnN BC1 using three different phenotypes (specific IgG, IL-6, and ankle swelling). *Bb6* on chromosome 12 was reproduced by two traits each in the F<sub>2</sub> intercross (total IgG and total IgM) and in the B6C3F<sub>1</sub> × C3H/HeN BC1 (tendon sheath thickness and total IgG). Another locus on chromosome 12, *Bb10*, was found using tendon sheath thickness and total IgG in the B6C3F<sub>1</sub> × C3H/HeN BC1. Two independent crosses, using different traits, also confirmed the *Bb12*, *Bb14*, and *Bb15* loci (see Table 2).

### Correlations between traits and their associated QTL

In the previously published analysis of the F<sub>2</sub> intercross, there were three cases (*Bb3*, *Bb5*, and *Bb6*) of two phenotypes linked to the same interval.<sup>11</sup> In each case, the correlation between the two traits linked to a single locus was highly significant ( $P < 0.0001$ , data not shown). This suggested that a single pleiotropic QTL influenced more than one phenotype, that the two measured phenotypes were both indicative of the overall disease process, or that two QTL influencing separate phenotypes were tightly linked. To better understand the linkage of two

phenotypes to a single locus, we examined the correlation of phenotypes in the BC1 populations.

In animals from the B6C3F<sub>1</sub> × C3H/HeN population, the correlation between the ankle swelling and histopathology score was high ( $\rho = 0.59$ ,  $P < 0.0001$ ). In this same B6C3F<sub>1</sub> × C3H/HeN BC1, the correlation between tendon sheath thickness and total IgG was not as high, even though both traits are linked to *Bb6* and *Bb10* ( $\rho = 0.25$ ,  $P = 0.0049$ ). Also in this same BC1 population, both specific IgG and IL-6 levels mapped to *Bb8* on chromosome 17 and displayed a high degree of correlation ( $\rho = 0.20$ ,  $P = 0.0045$ ). However, there are several other examples where highly correlated traits did not share the same susceptibility loci (data not shown, see Discussion).

### Resolution of *Bb2* and *Bb3* on chromosome 5

Using ankle swelling and histopathologic traits, *Bb2* was found in three of the BC1 populations as well as in the F<sub>2</sub> population. In each case, the *Bb2* allele causing increased severity came from the C3H/He (susceptible) parental strain (see Table 2). Additionally, *Bb2* was the only significant QTL in the (C3H/HeJ × BALB/cAnN) × C3H/HeJ BC1. Thus, the *Bb2* allele from C3H/He mice appears to be important for susceptibility to Lyme arthritis as revealed with four independent crosses involving three different mouse strains.

In an attempt to identify *Bb2*, we included markers for *Spp1* (osteopontin or *Eta1*) located at 56 cM, and *Cora1* at 73 cM in the genetic map to test them by CIM as candidate loci for *Bb2*. *Spp1* may affect the murine response to intercellular pathogens. For example, two different osteopontin deficient mice had impaired host defenses to intracellular pathogens, with one mouse more severely impaired than the second in IFN $\gamma$ -dependent events and granuloma formation.<sup>25,26</sup> *Cora1* is a second candidate locus at *Bb2* that was initially identified as a QTL linked to the correlated production of IL-4 and IL-10 after stimulation with ConA in (CcS-20 × BALB) F<sub>2</sub> hybrids.<sup>27</sup>

Inclusion of the markers for these candidate loci indicates that *Spp1* (as represented by *D5Mit115* at 56 cM), was excluded from the significance interval for *Bb2* in the BC1 populations. Maximal linkage of *Bb2* was found close to *D5Mit63* (the marker linked to *Cora1*) in the F<sub>2</sub> intercross and the three BC1 populations. Our linkage analyses with the reciprocal BC1 populations excluded

**Table 3** Location and effects of QTL controlling phenotypes in the F<sub>2</sub> intercross using CIM

QTL Designation	Phenotype	Chr	cM <sup>a</sup>	Marker <sup>b</sup>	LRT <sup>c</sup>	A <sup>d</sup>	D <sup>e</sup>	Var <sup>f</sup>
<i>Bb1</i>	Ankle swelling	4	28.6	<i>D4Mit139</i>	19.6	-0.163	0.041	8.4
<i>Bb2</i>	Ankle swelling	5	73.0	<i>D5Mit63</i>	18.7*	-0.064	-0.106	1.3
<i>Bb3</i>	Histopathology	5	53–60	<i>D5Mit91</i> – <i>D5Mit24</i>	25.1	-0.550	-0.119	10.5
<i>Bb4</i>	Histopathology	11	34.5	<i>D11Mit350</i>	18.8*	-0.519	0.154	9.9
<i>Bb5</i>	Specific IgM	6	71.6	<i>D6Mit200</i>	24.4	562.7	618.1	3.8
	Total IgM	6	43–67	<i>D6Mit230</i> – <i>D6Mit59</i>	29.2	156.7	-16.2	11.6
<i>Bb6</i>	Total IgG	12	52.0	<i>D12Mit139</i>	29.5	-221.7	-272.1	4.2
	Total IgM	12	52.0	<i>D12Mit139</i>	27.6	147.3	21.8	10.8
<i>Bb8</i>	Total IgG	17	22.5–23.3	<i>D17Mit176</i> – <i>215</i>	19.4	467.0	1162.7	2.9

<sup>a</sup>Distance according to MGD (<http://www.informatics.jax.org/>). <sup>b</sup>Marker(s) associated with linkage (passing the 95% permutation derived threshold for CIM). <sup>c</sup>LRT as in Table 2. \*Indicates linkage at 90% permutation-derived threshold. <sup>d</sup>Additive effect of the QTL relative to the C57BL/6 homozygote. A positive value indicates that the mean trait value for the C57BL/6 homozygotes is greater than the mean trait value for the heterozygous animals. <sup>e</sup>Dominance deviation. Deviation of the trait value for heterozygotes from the midpoint of the C57BL/6 and C3H/HeN homozygotes. <sup>f</sup>Percent variance accounted for by the QTL.

*Spp1* as a candidate gene, and suggested that *Cora1* may be a candidate locus.

*Bb2* and *Bb3*, both located on chromosome 5, were difficult to separate by CIM. In the analysis of the F<sub>2</sub> population by CIM with a window size of 10 cM, *Bb2* was confirmed at 60 cM (*D5Mit24*) using the trait of ankle swelling and *Bb3* was replicated at 53–60 cM (*D5Mit91–D5Mit24*) using the histopathology score (see Table 3). Thus, these highly correlated traits ( $P < 0.0001$ ) had significant QTL regions that overlapped on chromosome 5 and we were unable to differentiate the position and influence of *Bb2* and *Bb3*. Interestingly, this region from 53–60 cM is exclusively identified in the F<sub>2</sub> population (not the BC1 populations), and does include candidate gene and *Spp1*.

In the F<sub>2</sub> intercross, CIM with a window size of 5 cM gave maximal linkage to *D5Mit431* at 66 cM for histopathology score. The telomeric shift of the maximally linked marker as the window size decreased was due to the exclusion of a marker(s) and associated QTL at 5 cM or more from the test position. At *D5Mit431*, CIM with a 5 cM window excluded the effects of *D5Mit63* and *D5Mit24* as well as *D5Mit91*, and linkage may be due to an additional locus between *Bb2* and *Bb3* (see Table 4 and Figure 1). When a CIM with a 10 cM window was used, linkage was greatest when the testing window included the effects at both *D5Mit63* and *D5Mit91*. Additionally, tendon sheath thickness exhibits maximal linkage at 45 cM to *D5Mit312* (*Bb3*) when interval mapping or CIM is done with a 5 cM window. With a 10 cM window, CIM for tendon sheath thickness gives maximal linkage at *D5Mit312* when the test position does not exclude the influences at *D5Mit63* and *D5Mit91*, although it does not pass the 90% permutation threshold (data not shown).

In the (C3H/HeJ × BALB/cAnN) × C3H/HeJ BC1,

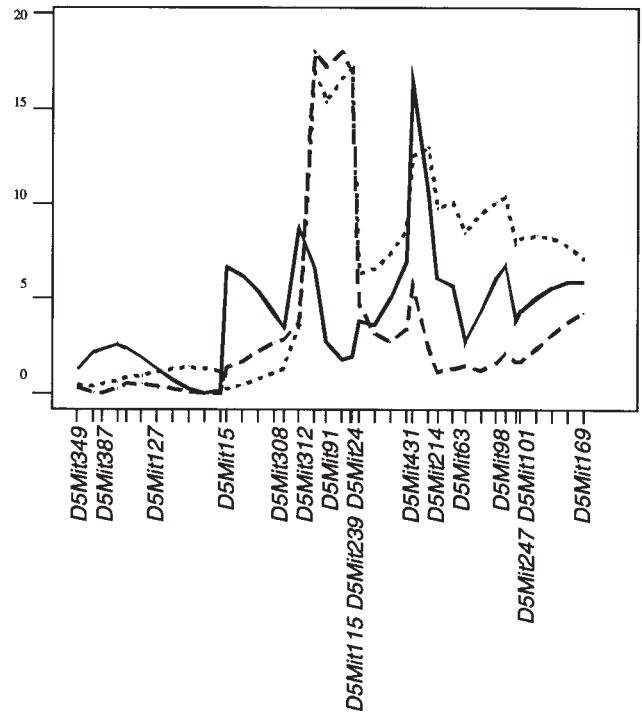


**Figure 1** CIM of the F<sub>2</sub> intercross on chromosome 5. CIM was performed using 20 background markers and a window size of 5 cM. The trait for ankle swelling is represented by the dotted line, histopathology score by the solid line and tendon sheath thickness by the dashed line.

**Table 4** LRT, markers, and intervals on chromosome 5 in the F<sub>2</sub> intercross population

Marker	MGD <sup>c</sup>	Position <sup>d</sup>	Tendon sheath thickness			Ankle swelling			Histopathology			
			IM <sup>e</sup>	CIM 10 cM <sup>f</sup>	CIM 5 cM <sup>g</sup>	IM <sup>e</sup>	CIM 10 cM <sup>f</sup>	CIM 5 cM <sup>g</sup>	IM <sup>e</sup>	CIM 10 cM <sup>f</sup>	CIM 5 cM <sup>g</sup>	
<i>D5Mit308</i> <sup>a</sup>	44	0.26	17.47	16.25	2.80	13.41	2.15	1.32	10.47	1.70	3.46	
			18.61	17.90	3.74	15.61	4.14	3.51	14.24	4.13	8.67	
<i>D5Mit312</i> <sup>a</sup>	45	0.30	18.59	18.59	17.91	16.48	3.71	16.89	16.94	6.64	6.64	
<i>D5Mit91</i> <sup>a</sup>	53	0.32	16.87	17.59	17.18	16.36	02.80	15.41	13.13	25.62	2.70	
			16.03	18.34	17.97	17.71	3.99	16.60	12.07	23.26	1.78	
<i>D5Mit115</i>	56	0.35	15.08	17.58	16.95	18.02	4.99	17.06	10.99	21.28	1.88	
<i>D5Mit239</i>	58	0.35	15.07	17.58	16.95	18.01	5.01	17.08	10.98	21.27	1.88	
<i>D5Mit24</i> <sup>b</sup>	60	0.36	13.63	17.49	4.70	16.86	18.52	6.35	9.75	20.36	3.84	
			0.38	14.51	19.78	3.13	18.16	21.76	6.59	11.84	25.10	3.62
			0.40	14.89	21.63	2.73	18.74	24.22	7.39	13.82	28.91	5.05
			0.42	14.64	22.56	3.34	18.54	26.01	8.60	15.44	31.84	7.00
<i>D5Mit431</i> <sup>b</sup>	66	0.43	14.36	5.15	5.70	18.27	10.67	12.52	15.97	7.76	16.37	
			0.45	11.45	2.34	2.48	17.92	10.21	12.90	13.01	4.91	10.58
<i>D5Mit214</i> <sup>b</sup>	70	0.46	9.20	1.15	1.13	16.51	11.03	9.82	10.85	6.06	6.06	
			0.48	10.03	1.10	1.33	18.74	11.24	10.05	11.97	5.63	5.63
<i>D5Mit63</i> <sup>b</sup>	73	0.49	10.17	0.99	1.44	18.74	10.04	8.54	11.74	4.52	2.68	
			0.51	9.72	1.35	1.25	18.35	11.67	9.50	11.11	6.61	4.35
			0.53	8.56	2.27	1.62	17.41	12.49	10.08	10.10	0.68	6.08
<i>D5Mit98</i> <sup>b</sup>	78	0.54	7.77	2.90	2.09	16.71	12.83	10.36	9.39	6.79	6.79	

<sup>a</sup>Markers included in original *Bb3* interval. <sup>b</sup>Markers included in original *Bb2* interval. <sup>c</sup>Published distance (in cM) from the centromere of the chromosome 5 according to MGD. <sup>d</sup>Test position. Markers are spaced according to recombination fractions detected in Mapmaker computer package. Two cM step intervals between marker positions are used in interval mapping (IM) and CIM in QTL Cartographer. <sup>e</sup>LRT using IM (model 3) of QTL Cartographer. <sup>f</sup>LRT using CIM (model 6) of QTL Cartographer with a 10 cM window. <sup>g</sup>LRT using CIM (model 6) of QTL Cartographer with a 5 cM window.

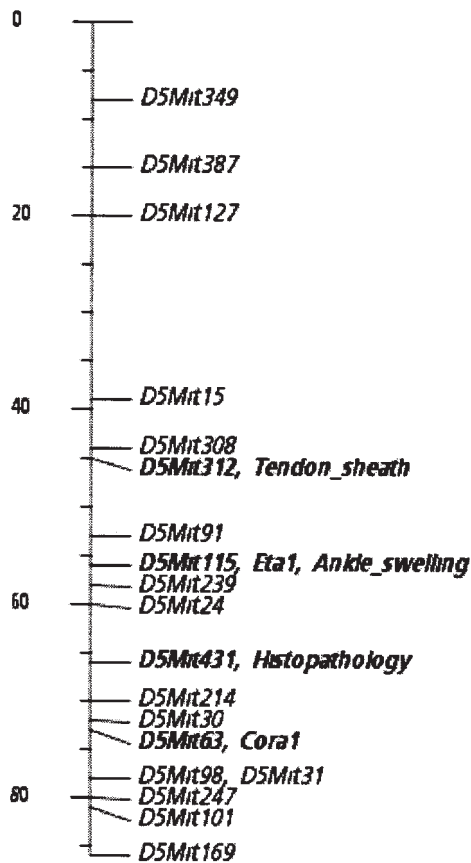


**Figure 2** Four putative QTL on chromosome 5. Microsatellite markers used in the  $F_2$  and BC1 populations are given with their distances according to MGD and not according to the recombination fractions between markers specifically generated for each cross. The marker order listed was replicated for each cross. Markers in bold letters identify the four putative QTL on chromosome 5. The tendon sheath thickness, ankle swelling and histopathology traits were localized using CIM with a 5 cM window using the  $F_2$  population. The *Cora1* locus was identified using ankle swelling and histology phenotypes from the reciprocal backcross populations. Map made using MapCreator (<http://www.wesbarris.com/mapcreator/mapcreator.html>).

CIM with a 10 cM window mapped histopathology and tendon histology to *Bb2*. Yet, the more centromeric side of the significant region for tendon histology is very close to *Bb3*. CIM with a 5 cM window places maximal linkage of tendon histology at 66 cM whereas maximal linkage for the histopathology score is at 72 cM. Once again, two distinct loci are linked to two different traits and this becomes clearer as the window size in CIM is changed. Taken together, our CIM analysis of  $F_2$  and BC1 populations provided evidence for at least three and possibly four loci controlling ankle swelling or histopathological responses to *B. burgdorferi* on chromosome 5. These loci are at 45, 53–60, 66 and 72–73 cM on chromosome 5 (see Figure 2). In future experiments, interval specific congenic lines across this region of chromosome 5 will be used to test this hypothesis.

## Discussion

Our analysis of the *B. burgdorferi*-infected reciprocal BC1 populations,  $B6C3F_1 \times C57BL/6N$ ,  $B6C3F_1 \times C3H/HeN$

and  $(C3H/HeJ \times BALB/cAnN) \times BALB/cAnN$  and  $(C3H/HeJ \times BALB/cAnN) \times C3H/HeJ$  identified 12 novel QTL and replicated three QTL from our previous genome scan.<sup>11</sup> We examined susceptible C3H/He mice crossed to two different resistant strains, C57BL/6N and BALB/cAnN, that may have different mechanisms of resistance.<sup>13</sup> We also reanalyzed the original  $F_2$  population using CIM, validating seven previously mapped QTL and identifying at least three additional *Bb* loci. Interestingly, three of the BC1 populations confirmed *Bb2* from the  $F_2$  intercross. In all cases, the C3H/He *Bb2* allele increased ankle swelling, tendon sheath thickness, and the severity of the histopathologic changes associated with arthritis. Therefore, the C3H/He allele at *Bb2* on chromosome 5 is very important in susceptibility to *B. burgdorferi*-induced phenotypes. The candidate locus *Cora1*, which appears to influence the ratio of IL-4 and IL-10, is particularly intriguing, given our recent finding of the importance of IL-10 in *B. burgdorferi*-induced lesions and the lack of effect of IL-4 and IL-13 on the development of Lyme arthritis.<sup>28,29</sup> IL-10 influences lesion severity and histopathology, and the ratio of IL-6 and TNF $\alpha$  to IL-10 may be important.<sup>12</sup> Thus *Bb2* may influence quantitative differences of the cytokine ratio, thereby affecting Lyme disease lesions.

Reanalysis of the  $F_2$  intercross using CIM provided additional resolution on chromosome 5 at the locations of *Bb2* and *Bb3*. By using different window sizes and examining the markers that were included and excluded, we saw evidence for four distinct QTL within a 30-cM region on chromosome 5 that affect ankle swelling and histopathologic phenotypes associated with experimentally induced Lyme arthritis. Two independent crosses derived from different parental combinations verified the existence of multiple QTL on chromosome 5 affecting different phenotypes. In analyses of mouse models of insulin-dependent diabetes mellitus (IDDM) and systemic lupus erythematosus (SLE), initial linkages to large intervals were later separated into two or more distinct loci by use of interval specific congenic mice.<sup>30–33</sup> Therefore, given the association of the three histologically scored phenotypes with different intervals exhibiting maximal linkage, our extended QTL analysis with CIM identified loci whose discovery otherwise may have required the use of interval specific congenic mice. The ability to detect three or more distinct QTL in the  $F_2$  intercross, and not in the BC1 populations, may be due to unique epistatic interactions that can only occur in this design. Alternatively, *Bb2* may only be important for susceptibility to ankle swelling and cellular changes that cause more severe histopathology in BC1 mice. Nevertheless, CIM provides important new information to be considered while generating congenic strains of mice that differ only in the region of the loci on chromosome 5.

The presence of multiple loci linked to different phenotypes on chromosome 5 was also supported by our correlation analysis. In both the  $F_2$  intercross and BC1 populations, when two traits were linked to the same locus, there was significant correlation between the traits. Yet, it is interesting to note that even though two phenotypes are highly correlated, they do not share linkage to all of the same QTL. Similar findings were seen by Lyons *et al* with IDDM.<sup>32</sup>

Our extended analysis of *Bb2* and *Bb3* and the examination of correlation of traits, illustrates that some QTL

may contain more than one gene related to the *B. burgdorferi* response. These multiple QTL may control a specific sub-phenotype, although these loci may be tightly linked and evolutionarily conserved. For example, our results indicate that the region from 45 to 81 cM on chromosome 5 contains multiple QTL governing the immunologic and pathologic sequelae associated with *B. burgdorferi* infection. Genes in this same region may also be important in responses to other infectious organisms. Four candidate genes, *Gro1* (51 cM), *Bmp3* (55 cM), *Spp1* (56 cM), and *Ibsp* (56 cM) and the candidate locus *Cora1* (73 cM) reside in this region. Conversely, the pleiotropic effects of a single gene, as seen in knockout mice, may affect more than one phenotype. Additional studies will help to distinguish between these two possibilities, although they may be unique to a particular locus.

In addition to replicating loci that were previously identified in the F<sub>2</sub> intercross, we have identified 14 new loci by taking into account the effect of background and tightly linked genes through CIM. For each phenotype tested, the strains that developed severe arthritis and had a higher humoral response were C3H/HeN and C3H/HeJ and those that developed mild arthritis and had a lower magnitude humoral response were C57BL/6N or BALB/cAnN (see Table 1). Eight of the eleven linkages identified using the B6C3F<sub>1</sub> × C3H/HeN BC1 had two alleles from C3H/HeN mice that increased trait severity. *Bb10* and *Bb11* displayed a heterozygous effect (see Table 2), and at *Bb10*, this was the case with two correlated traits. In the B6C3F<sub>1</sub> × C57BL/6N BC1, six of nine linkages were due to homozygous C57BL/6N alleles. Of interest, *Bb15*, mapped in both B6C3F<sub>1</sub> × C3H/HeH and B6C3F<sub>1</sub> × C57BL/6N BC1 populations, was found in each case because of homozygosity of the recurrent parent of backcross. Detection of this locus in our previous study had been obscured in the F<sub>2</sub> cross and possibly by the presence of two QTL in this region.<sup>34</sup>

Similar confirmations of important disease-causing alleles and identification of additional alleles have been seen when the same parental strains were used in BC1 and F<sub>2</sub> populations studying experimental allergic encephalomyelitis (EAE)<sup>35–37</sup> and in murine models of SLE.<sup>38–42</sup> Yet, we have found no study that has used both reciprocal BC1 populations and an F<sub>2</sub> derived from the same inbred strains to identify and replicate QTL. The advantage of using reciprocal BC1 and F<sub>2</sub> intercross populations to detect QTL controlling murine Lyme disease may be due to the fact that C3H/HeJ and C57BL/6N mice exhibit significant differential susceptibility for each phenotype tested, with C3H/He always being more susceptible. Additionally, the animals were bred and infected under the same conditions, thus controlling for many environmental effects and the markers used in the genome scan were the same in each cross with little variation. Even though the maps that were generated for each cross were slightly different, use of the same markers was very important in the direct comparison of loci and the markers used to represent the background in CIM.

Additionally, our use of two additional BC1 populations between the susceptible C3H/He and BALB/c strains is also enlightening given the history of the C3H strain. C3H was derived from a cross between Bagg Albino mice (predecessor to the BALB mice strain) and DBA mice in 1920.<sup>43</sup> Because the offspring were selected

for tumor development, it would be expected that they would not carry 50% of each of the genomes of the parents. Given our difficulty in finding polymorphic microsatellite markers between C3H/He and BALB/c covering the entire genome at 20-cM intervals (see Materials and methods), we assume that regions of high homozygosity exist between the two strains. Despite these regions of homozygosity and relatedness of C3H/He and BALB/c, we were able to identify seven QTL in our reciprocal BC1 populations. Only one of the QTL was unique (*Bb20*), and is the result of homozygous alleles from BALB/cAnN (resistant) mice (see Table 2). Because BALB/c mice appear to have a different mechanism of resistance than C57BL/6 to infection with *B. burgdorferi*,<sup>13</sup> and because a different *B. burgdorferi* strain was used in BALB/c BC1 backcrosses, the loci found in BC1 with BALB/c may be unique to that mechanism of resistance or to the strain of pathogen used. Nevertheless, the additional information found using the reciprocal BC1 between C3H/HeJ and BALB/cAnN mice verified significant QTL on chromosomes 5, 15, and 17, suggesting that there is a high probability of finding candidate genes in a region common to independent crosses, especially when related strains are used.

Mice with different genetic backgrounds may harbor different susceptibility genes even though they may not cause susceptibility in a particular strain of mice. Inbred strains showing resistance to *B. burgdorferi* infection also contain susceptibility loci and these loci may be unmasked only when they interact with loci from a susceptible strain. Because QTL differ from Mendelian traits, cross-specific information may be uniquely identified.

By using F<sub>2</sub> and reciprocal BC1 populations between susceptible C3H/He and resistant C57BL/6N and BALB/cAnN mice, we have shown that the susceptibility of *B. burgdorferi*-induced Lyme arthritis in mice is complex and polygenic in nature. The genetic control of the nine different intermediate phenotypes is due to at least 23 different loci on 14 different chromosomes. The isolation and identification of the major QTL may provide direct insight into the interesting relationships between these intermediate phenotypes and the pathways leading to immunologic and pathologic sequelae.

## Materials and methods

### Mice

C3H/HeN, C57BL/6N, BALB/cAnN and B6C3F<sub>1</sub> (C3H/HeN × C57BL/6N) mice were obtained from the National Cancer Institute. A total of 84 B6C3F<sub>1</sub> × C57BL/6N, 194 B6C3F<sub>1</sub> × C3H/HeN and 136 (C3H/HeJ × BALB/cAnN) × BALB/cAnN, 96 (C3H/HeJ × BALB/cAnN) × C3H/HeJ reciprocal BC1 mice were bred and housed in the Animal Resource Center at the University of Utah Medical Center, according to guidelines of the National Institutes of Health for the care and use of laboratory animals.

### Infection

For infection of the B6C3F<sub>1</sub> × C3H/HeN and B6C3F<sub>1</sub> × C57BL/6N mice, *B. burgdorferi*, at passage 3 from an infected mouse, was obtained from Dr Stephen Barthold (University of California at Davis). *B. burgdorferi* was subsequently grown in BSK-H medium with 6%

rabbit serum (Sigma, St Louis, MO, USA). Spirochetes were counted in a Petroff-Hauser chamber and subsequently diluted into sterile medium. Five- to 7-week-old BC1 (194 B6C3F1 × C3H/HeN, 84 B6C3F1 × C57BL/6N) mice were infected by intradermal injection on a shaved back with  $2 \times 10^3$  spirochetes from passage 5 of the N40 isolate of *B. burgdorferi*. For infection of the (C3H/HeJ × BALB/cAnN) × BALB/cAnN and (C3H/HeJ × BALB/cAnN) × C3H/HeJ mice, the HB19 isolate of *B. burgdorferi* was provided by Dr Alan Barbour (University of California at Irvine). A total of 136 (C3H/HeJ × BALB/cAnN) × BALB/cAnN and 96 (C3H/HeJ × BALB/cAnN) × C3H/HeJ mice (a mixture of male and female) were infected by intradermal injection on a shaved back with  $2 \times 10^4$  spirochetes. Control C3H/HeN, C3H/HeJ, C57BL/6N, BALB/cAnN, B6C3F1 and (C3H/HeJ × BALB/cAnN) F1 mice were also infected by use of the corresponding protocols (see Table 1). The infection was followed for 4 weeks, after which the mice were killed. Mice were measured for histological and humoral phenotypes that have previously been shown to be important in disease.<sup>4,5,13,15–17</sup>

#### Detection of *B. burgdorferi* specific and total circulating immunoglobulin levels, and detection of serum IL-6

Serum samples, taken from infected and control mice killed 4 weeks after infection, were analyzed for *B. burgdorferi*-specific antibody and for total circulating IgG and IgM by a quantitative antibody capture ELISA as described elsewhere.<sup>11</sup> IL-6 levels in serum were assayed by antibody capture ELISA using rat anti-mouse IL-6 monoclonal antibody pairs and recombinant mouse IL-6 standard from Pharmingen (San Diego, CA, USA).<sup>16</sup>

#### Measurement of the ankle joints

Rear ankle joints of mice were measured with a metric caliper (Mitutoyo, Japan) at death. Measurements were taken in the anterior/posterior position, with the ankle extended, which was through the thickest portion of the ankle. Normal ankle joints have a diameter of approximately 3 mm at this position, with measurements up to 4.5 mm observed in severely arthritic mice.

#### Histopathology of ankle joints

When mice were killed 4 weeks after infection, the rear ankle joint with the greatest swelling was taken from each mouse for histological analysis, as described elsewhere.<sup>11</sup> A score of 4 indicated the greatest severity in tissues of the ankle and tibia: a large region of edema with presence of many neutrophils, thickening of the tendon sheath, and evidence of bone and cartilage abnormalities within the tendon sheath. A score of 1 displayed slight thickening of the tendon sheath, and little edema and neutrophil infiltration; a score of 0 was given to samples indistinguishable from mock-infected controls. Scores of 2 and 3 were assigned to samples with intermediate lesion severity. A similar evaluation assigned a score of 0–4 for tendon sheath histology.

A second quantification of histopathological severity was obtained by measurement of the thickness of the tendon sheath of the cranial tibial muscle as previously described.<sup>11</sup> The average of four measurements made at approximately equal spacing was used for QTL analysis.

#### Quantitation of *B. burgdorferi* DNA in mouse tissues

*B. burgdorferi* DNA levels were determined in DNA prepared from hearts of infected BC1, F<sub>1</sub>, F<sub>2</sub> and parental mice by continuous monitoring polymerase chain reaction (PCR) using the Light Cycler (Idaho Technologies, Idaho Falls, ID, USA).<sup>44</sup>

#### Genotyping of BC1 mice

We constructed genetic linkage maps of the mouse genome for each individual BC1. Genomic DNA was isolated from rear ankle joints. Maps were made using 194 C3H/HeN × B6C3F1 and 84 C57BL/6N × B6C3F1 mice. One hundred and ninety-five microsatellite markers that discriminated between C3H/He and C57BL/6 alleles were used to scan all chromosomes of the mouse genome; distances between markers or on the ends of a single chromosome did not exceed 20 cM. Maps for BALB/c crosses were made using 136 (C3H/HeJ × BALB/cAnN) × BALB/cAnN and 96 (C3H/HeJ × BALB/cAnN) × C3H/HeJ mice with 111 and 115 microsatellite markers, respectively, that distinguished between the C3H/He and the BALB/c alleles. A map with 20-cM resolution for these BC1 populations was not achieved. Some regions had no resolvable polymorphisms between C3H and BALB, we suspect this is due to the close relationship between C3H and BALB<sup>43</sup> (see Discussion). Microsatellite primers were either purchased from Research Genetics (Huntsville, AL, USA) or synthesized according to sequences obtained through the Whitehead Institute/MIT mouse genome database ([www.genome.wi.mit.edu/cgi-bin/mouse/index](http://www.genome.wi.mit.edu/cgi-bin/mouse/index)). PCR parameters for microsatellite typing were as described elsewhere.<sup>45</sup> Microsatellite size variants were resolved by electrophoresis on large format denaturing 7% polyacrylamide gels and visualized by autoradiography.

#### QTL analysis

Linkage maps were estimated using MAPMAKER/EXP computer package and a Kosambi map function.<sup>46,47</sup> CIM was used for localization of QTL using model 6 of the Zmapqtl program in QTL Cartographer program (<http://statgen.ncsu.edu/qtlcart/cartographer.html>).<sup>48</sup> CIM combines classical interval mapping with multiple regression, and, as such, it permits a more precise definition of QTL location, controls for spurious ghost loci, and allows the detection of more than one QTL on a chromosome.<sup>20–24,49</sup> To choose background markers for CIM, a linear regression model with a forward/backward selection procedure was run in the SRmapqtl module of QTL Cartographer. These background markers are of two types: markers flanking the test interval to control for the presence of linked QTL on the chromosome examined, and markers unlinked to the test interval but with significant effects on the trait. An initial window size of 10 cM (and later 5 cM) was used to define the flanking markers, and CIM was performed in 2 cM increments. Twenty background markers were used in the F<sub>2</sub> intercross, 10 background markers were used in the BC1 between C3H and C57BL/6 mice, and five background markers were used with the BC1 between C3H and BALB/c mice. The number of background markers was chosen by considering the number of significant linkages found using interval mapping (model 3) and the number of microsatellite markers included in the cross. Tests of significant linkage for a QTL are reported in the form of



a likelihood ratio test (LRT) statistic (LOD = LRT × (0.2171)). All marker locations and putative QTL are given as distances from the centromere of the acrocentric mouse chromosome as found in the Mouse Genome Database (MGD: <http://www.informatics.jax.org>).

### Permutation derived critical values

QTL Cartographer was employed to assess the significance of the linkage between marker loci and putative QTL via permutation-based threshold analysis.<sup>49,50</sup> Significant ( $\alpha = 0.05$ ) and suggestive ( $\alpha = 0.10$ ) experimentwise critical values were determined using the distribution of maximum LRT statistics from 1000 permutations of our data.

### Acknowledgements

We are grateful to Dr Lei Liu and Keith Frazier of the Bioinformatics Unit of the W.M. Keck Center for Comparative and Functional Genomics at the University of Illinois at Urbana-Champaign for O2K computer resources, and also Mark Clement of Brigham Young University for computer support.

### References

- 1 Orloski KA, Hayes EB, Campbell GL, Dennis DT. Surveillance for Lyme disease—United States. *Mor Mortal Wkly Rep CDC Surveill Summ* 2000; **49**: 1–11.
- 2 Burgdorfer W, Barbour AG, Hayes SF, Benach JL, Grunwaldt E, Davis JP. Lyme disease—a tick-borne spirochetosis? *Science* 1982; **216**: 1317–1319.
- 3 Nocton JJ, Steere AC. Lyme disease. *Adv Intern Med* 1995; **40**: 69–117.
- 4 Simon MM, Schaible UE, Wallich R, Kramer MD. A mouse model for *Borrelia burgdorferi* infection: approach to a vaccine against Lyme disease. *Immunol Today* 1991; **12**: 11–16.
- 5 Golde WT, Kappel KJ, Dequesne G *et al*. Tick transmission of *Borrelia burgdorferi* to inbred strains of mice induces an antibody response to P39 but not to outer surface protein A. *Infect Immun* 1994; **62**: 2625–2627.
- 6 Steere AC, Schoen RT, Taylor E. The clinical evolution of Lyme arthritis. *Ann Intern Med* 1987; **107**: 725–731.
- 7 Nocton JJ, Dressler F, Rutledge BJ *et al*. Detection of *Borrelia burgdorferi* DNA by polymerase chain reaction in synovial fluid from patients with Lyme arthritis. *N Engl J Med* 1994; **330**: 229–234.
- 8 Gross DM, Forsthuber T, Tary-Lehmann M *et al*. Identification of LFA-1 as a candidate autoantigen in treatment-resistant Lyme arthritis. *Science* 1998; **281**: 703–706.
- 9 Hemmer B, Gran B, Zhao Y *et al*. Identification of candidate T-cell epitopes and molecular mimics in chronic Lyme disease. *Nat Med* 1999; **5**: 1375–1382.
- 10 Barthold SW, Beck DS, Hansen GM, Terwilliger GA, Moody KD. Lyme borreliosis in selected strains and ages of laboratory mice. *J Infect Dis* 1990; **162**: 133–138.
- 11 Weis JJ, McCracken BA, Ma Y *et al*. Identification of quantitative trait loci governing arthritis severity and humoral responses in murine model of Lyme disease. *J Immunol* 1999; **162**: 948–956.
- 12 Wooten RM, Weis JJ. Host-pathogen interactions promoting inflammatory Lyme arthritis: use of mouse models for dissection of disease processes. *Curr Opin Microb* 2001; **4**: 274–279.
- 13 Ma Y, Seiler KP, Eichwald EJ, Weis JH, Teuscher C, Weis JJ. Distinct characteristics of resistance to *Borrelia burgdorferi*-induced arthritis in C57BL/6N mice. *Infect Immun* 1998; **66**: 161–168.
- 14 Armstrong AL, Barthold SW, Persing DH, Beck DS. Carditis in Lyme disease susceptible and resistant strains of laboratory mice infected with *Borrelia burgdorferi*. *Am J Trop Med Hyg* 1992; **47**: 249–258.

- 15 Schaible UE, Kramer MD, Wallich R, Tran T, Simon MM. Experimental *Borrelia burgdorferi* infection in inbred mouse strains: antibody response and association of H-2 genes with resistance and susceptibility to development of arthritis. *Eur J Immunol* 1991; **21**: 2397–2405.
- 16 Yang L, Ma Y, Schoenfeld R *et al*. Evidence for B-lymphocyte mitogen activity in *Borrelia burgdorferi*-infected mice. *Infect Immun* 1992; **60**: 3033–3041.
- 17 Matyniak JE, Reiner SL. T helper phenotype and genetic susceptibility in experimental Lyme disease. *J Exp Med* 1995; **181**: 1251–1254.
- 18 Barthold SW, Sidman CL, Smith, AL. Lyme borreliosis in genetically resistant and susceptible mice with severe combined immunodeficiency. *Am J Trop Med Hyg* 1992; **47**: 605–613.
- 19 Brown CR, Reiner SL. Genetic control of experimental Lyme arthritis in the absence of specific immunity. *Infect Immun* 1999; **67**: 1967–1973.
- 20 Zeng ZB. Precision mapping of quantitative trait loci. *Genetics* 1994; **136**: 1457–1468.
- 21 Zeng ZB. Theoretical basis for separation of multiple linked gene effects in mapping quantitative trait loci. *Proc Natl Acad Sci USA* 1993; **90**: 10972–10976.
- 22 Teuscher C, Butterfield RJ, Ma RZ, Zachary JF, Doerge RW, Blankenhorn EP. Sequence polymorphisms in the chemokines Scya1 (TCA-3), Scya2 (monocyte chemoattractant protein (MCP)-1), and Scya12 (MCP-5) are candidates for eae7, a locus controlling susceptibility to monophasic remitting/nonrelapsing experimental allergic encephalomyelitis. *J Immunol* 1999; **163**: 2262–2266.
- 23 Butterfield RJ, Blankenhorn EP, Roper RJ, Zachary JF, Doerge RW, Teuscher C. Identification of genetic loci controlling the characteristics and severity of brain and spinal cord lesions in experimental allergic encephalomyelitis. *Am J Pathol* 2000; **157**: 637–645.
- 24 Ewart SL, Kuperman D, Schadt E *et al*. Quantitative trait loci controlling allergen-induced airway hyperresponsiveness in inbred mice. *Am J Respir Cell Mol Biol* 2000; **23**: 537–545.
- 25 Nau GJ, Liaw L, Chupp GL, Berman JS, Hogan BL, Young RA. Attenuated host resistance against *Mycobacterium bovis* BCG infection in mice lacking osteopontin. *Infect Immun* 1999; **67**: 4223–4230.
- 26 Ashkar S, Weber GF, Panoutsakopoulou V *et al*. Eta-1 (osteopontin): an early component of type-1 (cell-mediated) immunity. *Science* 2000; **287**: 860–864.
- 27 Kosarova M, Havelkova H, Krulova M, Demant P, Lipoldova M. The production of two Th2 cytokines, interleukin-4 and interleukin-10, is controlled independently by locus *Cypr1* and by loci *Cypr2* and *Cypr3*, respectively. *Immunogenetics* 1999; **49**: 134–141.
- 28 Brown JP, Zachary JF, Teuscher C, Weis JJ, Wooten RM. Dual role of interleukin-10 in murine Lyme disease: regulation of arthritis severity and host defense. *Infect Immun* 1999; **67**: 5142–5150.
- 29 Potter MR, Noben-Trauth N, Weis JH, Teuscher C, Weis JJ. Interleukin-4 (IL-4) and IL-13 signaling pathways do not regulate *Borrelia burgdorferi*-induced arthritis in mice: IgG1 is not required for host control of tissue spirochetes. *Infect Immun* 2000; **68**: 5603–5609.
- 30 Wicker LS, Todd JA, Prins JB, Podolin PL, Renjilian RJ, Peterson LB. Resistance alleles at two non-major histocompatibility complex-linked insulin-dependent diabetes loci on chromosome 3, *Idd3* and *Idd10*, protect nonobese diabetic mice from diabetes. *J Exp Med* 1994; **180**: 1705–1713.
- 31 Podolin PL, Denny P, Lord CJ *et al*. Congenic mapping of the insulin-dependent diabetes (*Idd*) gene, *Idd10*, localizes two genes mediating the *Idd10* effect and eliminates the candidate *Fcgr1*. *J Immunol* 1997; **159**: 1835–1843.
- 32 Lyons PA, Hancock WW, Denny P *et al*. The NOD *Idd9* genetic interval influences the pathogenicity of insulinitis and contains molecular of *Cd30*, *Tnfr2*, and *Cd137*. *Immunity* 2000; **13**: 107–115.

- 33 Wakeland EK, Wandstrat AE, Liu K, Morel L. Genetic dissection of systemic lupus erythematosus. *Curr Opin Immunol* 1999; **11**: 701–707.
- 34 Butterfield RJ, Roper RJ, Rhein DM *et al*. Sex specific QTL govern susceptibility to Theiler's murine encephalomyelitis virus-induced demyelination (TMEVD). (submitted for publication).
- 35 Encinas JA, Lees MB, Sobel RA *et al*. Genetic analysis of susceptibility to experimental autoimmune encephalomyelitis in a cross between SJL/J and B10.S mice. *J Immunol* 1996; **157**: 2186–2192.
- 36 Butterfield RJ, Sudweeks JD, Blankenhorn EP *et al*. New genetic loci that control susceptibility and symptoms of experimental allergic encephalomyelitis in inbred mice. *J Immunol* 1998; **161**: 1860–1867.
- 37 Blankenhorn EP, Butterfield RJ, Rigby R *et al*. Genetic analysis of the influence of pertussis toxin on experimental allergic encephalomyelitis susceptibility: an environmental agent can override genetic checkpoints. *J Immunol* 2000; **164**: 3420–3425.
- 38 Kono DH, Burlingame RW, Owens DG *et al*. Lupus susceptibility loci in New Zealand mice. *Proc Natl Acad Sci USA* 1994; **91**: 10168–10172.
- 39 Morel L, Rudofsky UH, Longmate JA, Schiffenbauer J, Wakeland EK. Polygenic control of susceptibility to murine systemic lupus erythematosus. *Immunity* 1994; **1**: 219–229.
- 40 Vyse TJ, Morel L, Tanner FJ, Wakeland EK, Kotzin BL. Backcross analysis of genes linked to autoantibody production in New Zealand White mice. *J Immunol* 1996; **157**: 2719–2727.
- 41 Vyse TJ, Rozzo SJ, Drake CG, Izui S, Kotzin BL. Control of multiple autoantibodies linked with a lupus nephritis susceptibility locus in New Zealand black mice. *J Immunol* 1997; **158**: 5566–5574.
- 42 Vyse TJ, Kotzin BL. Genetic susceptibility to systemic lupus erythematosus. *Annu Rev Immunol* 1998; **16**: 261–292.
- 43 Festing MFW. Inbred strain characteristics ([http://www.informatics.jax.org/external/festing/search\\_form.cgi](http://www.informatics.jax.org/external/festing/search_form.cgi)).
- 44 Morrison TB, Ma Y, Weis JH, Weis JJ. Rapid and sensitive quantification of *Borrelia burgdorferi*-infected mouse tissues by continuous fluorescent monitoring of PCR. *J Clin Microbiol* 1999; **37**: 987–992.
- 45 Sudweeks JD, Todd JA, Blankenhorn EP *et al*. Locus controlling Bordetella pertussis-induced histamine sensitization (Bphs), an autoimmune disease-susceptibility gene, maps distal to T-cell receptor beta-chain gene on mouse chromosome 6. *Proc Natl Acad Sci USA* 1993; **90**: 3700–3704.
- 46 Lander ES, Green P, Abrahamson J *et al*. MAPMAKER: an interactive computer package for constructing primary genetic linkage maps of experimental and natural populations. *Genomics* 1987; **1**: 174–181.
- 47 Lincoln S, Daly M, Lander E. *Constructing Genetic Maps With MAPMAKER/EXP 3.0*. Whitehead Institute Technical Report. 3rd edition, 1992.
- 48 Basten CJ, Weir BS, Zeng ZB. *QTL Cartographer: A Reference Manual and Tutorial for QTL Mapping*. Department of Statistics, North Carolina State University, Raleigh, NC, 1997.
- 49 Doerge RW, Zeng ZB, Weir BS. Statistical issues in the search for genes affecting quantitative traits in experimental populations. *Stat Sci* 1997; **12**: 195–219.
- 50 Churchill GA, Doerge RW. Empirical threshold values for quantitative trait mapping. *Genetics* 1994; **138**: 963–971.